



# Evaluation and projected changes in daily rainfall characteristics over Central Africa based on a multi-model ensemble mean of CMIP5 simulations

Denis Sonkoué<sup>1</sup> · David Monkam<sup>2</sup> · Thierry C. Fotso-Nguemo<sup>1,3</sup> · Zéphirin D. Yepdo<sup>1,3</sup> · Derbetini A. Vondou<sup>1</sup>

Received: 5 July 2018 / Accepted: 25 November 2018 / Published online: 6 December 2018  
© Springer-Verlag GmbH Austria, ein Teil von Springer Nature 2018

## Abstract

This study uses daily rainfall data from 20 global climate models (GCMs) simulations, participating in the phase 5 of the Coupled Model Intercomparison Project (CMIP5) and eight daily rainfall indices defined by the Expert Team on Climate Change Detection and Indices (ETCCDI), to investigate the changes in extreme weather conditions over Central Africa under the representative concentration pathway 8.5. The performance of the multi-model ensemble (MME) mean which in fact refers to the best performing models selected through the Taylor diagram analysis was evaluated by comparing with two gridded daily observation datasets during the historical period (1998–2005). Results show that although some uncertainties may exist between the gridded observation datasets, MME consistently outperform individual models and reasonably reproduced the observed pattern of daily rainfall indices over the region, except in the case of consecutive wet day (CWD) where the high variability of individual members has resulted in the degradation of the overall skill of the MME. The assessment of the climate change signal in the eight daily rainfall indices was done for the mid and late twenty-first century (2026–2056 and 2066–2095 respectively), relative to the baseline historical time period (1976–2005). We found a significant increase in the total wet day rainfall amount (PRCPTOT) over southern (northern) Central Africa from December to February (from September to November). This is mainly due to the increase of high intense rainfall events rather than their frequency. The results also reveal that the increase in PRCPTOT was coupled with increase in the maximum consecutive 5-day rainfall amount (RX5DAY), the 95th percentile (R95), and the total wet day rainfall amount above the 95th percentile (R95PTOT), with more robust patterns of change at the late twenty-first century. The increase in extreme rainfall events (RX5DAY, R95, and R95PTOT) is likely to increase flood risks over Cameroon, Central African Republic, Gabon, Congo, Angola, Zambia, and Democratic Republic of Congo. On the other hand, changes in CWD and PRCPTOT are projected to significantly decrease over Angola, Zambia, and Democratic Republic of Congo from September to November. This is due to a substantial increase of zonal moisture divergence fluxes in upper atmospheric layers. The analysis has also shown that areas where CWD and PRCPTOT decreases coincides with those where consecutive dry days (CDD) increase. The decrease in CWD and PRCPTOT coupled with the increase in CDD could worsen drought risk and significantly disrupt priority socio-economic sectors for development such as rain-fed agriculture, hydroelectric power generation, and water resource availability. The results thus underline the importance for decision-makers to seriously consider adaptation and mitigation measures, in order to limit the risks of natural disasters such as severe droughts and floods that Central African countries may suffer in the future.

## 1 Introduction

Changes in future extreme rainfall events at the mid- and the end of the twenty-first century are projected to have negative

effects on the vulnerable biodiversity of the African continent. According to the Fifth Assessment Reports (AR5) of the Intergovernmental Panel on Climate Change (IPCC), the evidence of climate change is nowadays a challenge, because of natural disasters such as severe droughts and flooding linked to extreme weather events that may cause stress in water resource availability (IPCC 2013). The rapid increase of greenhouse gas (GHG) concentrations in the atmosphere, mainly due to human activities, is considered by the scientific community as the main driver causing these changes.

✉ Denis Sonkoué  
sonkouedenis@yahoo.fr

Extended author information available on the last page of the article.

The impact in the global process of climate change is not the same across regions of the world (Trenberth 2011). Particularly, Central Africa which highly depends on rain-fed agriculture, breeding, and hydroelectric power generation as the main source of its economy (Sonwa et al. 2012) is not spared by the adverse effects of climate change. Each year, this region experiences the highest number of natural and human-induced disasters in all of Africa (FAO 2018). In this region, the lack of infrastructure and the low adaptive capacity contribute to amplify the impact of extreme weather conditions which often have dramatic consequences (Almer et al. 2017). It is the case of the landslides caused by consecutive 7-day rainfall coupled with flooding that occurred at Magha, Batibo, and Bafou (Cameroon) on July 20, 2003, where 25 people perish and cause enormous economic losses (Zogning et al. 2007). Similar extreme events most often related to floods/droughts have also been reported in several major cities of Central African countries (Saha 2015; Tanessong et al. 2017). So, assessing rainfall pattern characteristics and possible future changes in this particular region can provide outline to policy makers for mitigation strategies and disaster risk management (Alsdorf et al. 2016; Aloysius and Saiers 2017; Pokam MW et al. 2018b).

Given these important socio-economic dangers, a particular interest has gradually been brought to the attention of extreme weather conditions in Africa. Some of these studies have used in situ or reanalysis datasets and found the significant increase/decrease in the magnitude and trends of extreme rainfall events (e.g., Fauchereau et al. 2003; Kruger 2006; Aguilar et al. 2009; Chamani et al. 2018). On the other hand, the results of climate models are rather mixed and vary according to the studied African sub-region, the climate change scenario used, or the type of model used (e.g., Vizy and Cook 2012; Sylla et al. 2015; Diallo et al. 2016; Abiodun et al. 2017; Fotso-Nguemo et al. 2018; Pokam et al. 2018a; Nikulin et al. 2018; Akinsanola and Zhou 2018b; Libanda and Ngonga 2018).

Today, there are only few studies devoted to the extreme weather conditions in Central Africa (Aguilar et al. 2009; Haensler et al. 2013; Fotso-Nguemo et al. 2018; Pokam et al. 2018a; Libanda and Ngonga 2018). Although the regional climate models (RCMs) archived as part of the COordinated Regional climate Downscaling EXperiment (CORDEX; <http://www.cordex.org>) initiative disagree in simulating mean rainfall changes across the region, there is tendency towards decrease of seasonal rainfall and reduction of consecutive wet days at the 1.5 °C and 2 °C global warming levels (Pokam et al. 2018a). Recently, based on a combined set of RCMs and global climate models (GCMs) from the phase 5 of the Coupled Model Intercomparison Project (CMIP5; <https://cmip.llnl.gov/cmip5/>), Haensler et al. (2013) investigated the changes

in the annual total rainfall and in the intensity of heavy rainfall events. Their results highlight the increase in the intensity of heavy rainfall events for both high and low GHG emission scenarios. Using an ensemble mean of best performing GCMs simulations, Fotso-Nguemo et al. (2018) found that there is an increasing trend in the annual heavy rainfall events across Central Africa. They suggest that this trend can be linked to the increase of moisture convergence intensified by the presence of the Congo Basin rainforest. To better understand rainfall characteristics using in situ dataset, Aguilar et al. (2009) have analyzed the annual trend in some rainfall indices over three African regions including Central Africa. Their analysis revealed that while the majority of the analyzed world has shown an increase in heavy rainfall events during the last half of the twentieth century, Central Africa showed a decrease in heavy rainfall events.

However, although the assessment of changes in extreme weather events is done over the Central African region, most of these studies only analyze either a single data source or a large ensemble of all available models. In addition, the method used to select the best performing models is sometimes only based on average rainfall and therefore can be subject to the uncertainties brought by different interpretations, depending on the choice of the data source or the type of the ensemble used. It would therefore be interesting to first select the models that simulate the different studied rainfall indices in a realistic way and then use their ensemble mean to assess the climate change signal of extreme weather events in the region.

In this work, we propose to use eight rainfall indices to firstly evaluate the capability of an ensemble mean of best performing GCMs simulations in representing recent past (1998–2005) daily rainfall characteristics and, secondly present their projected changes over Central Africa through the twenty-first century under global warming. This work has the particularity to explore large number of rainfall indices with a focus not only on the annual rainfall trends but on all the different seasons of the region. Moreover, the methodology used to quantify the uncertainties in the climate change signal allows us to hope in providing meaningful projections for the future. The paper is structured as follows: Section 2 outlines the data and methodologies used. Section 3 is devoted to the main results and discussion. Summary and conclusions are provided in Section 4.

## 2 Data and methodology

For analysis, daily rainfall data from 20 available GCMs produced during the CMIP5 experiment are used (see, Table 1). These GCMs spanning the period from 1850 to 2100 are subdivided as follows: 1850 to 2005 represents the recent past or historical, and 2006 to 2100 represents the

**Table 1** Summary of the 20 GCMs simulations used

Model name	Institute ID	Lat × lon
1 ACCESS1-0	Commonwealth Scientific and Industrial Research Organisation and Bureau of Meteorology, Australia	1.875° × 1.25°
2 BCC-CSM1-1-M	Beijing Climate Center (BCC), China Meteorological Administration, China	2.8° × 2.8°
3 BNU-ESM	College of Global Change and Earth System Science, Beijing Normal University	2.8° × 2.8°
4 CanESM2	Canadian Centre for Climate Modelling and Analysis, Victoria, BC, Canada	2.8° × 2.8°
5 CMCC-CESM	CMCC - Centro Euro-Mediterraneo per i Cambiamenti Climatici, Bologna, Italy	3.75° × 3.75°
6 CNRM-CM5	Centre National de Recherches Meteorologiques, Meteo-France, Toulouse, France	1.4° × 1.4°
7 CSIRO-Mk3-6-0	Commonwealth Scientific and Industrial Research Organization	1.875° × 1.875°
8 EC-EARTH	European Earth System Model	1.125° × 1.125°
9 GFDL-CM3	Geophysical Fluid Dynamics Laboratory	2.5° × 2.0°
10 GFDL-ESM2G	Geophysical Fluid Dynamics Laboratory	2.5° × 2.0°
11 GFDL-ESM2M	Geophysical Fluid Dynamics Laboratory	2.5° × 2.0°
12 HadGEM2-ES	Met Office Hadley Centre, Fitzroy Road, Exeter, Devon, EX1 3PB, UK	1.875° × 1.25°
13 IPSL-CM5A-LR	Institut Pierre Simon Laplace, Paris, France	3.75° × 1.8°
14 IPSL-CM5A-MR	Institut Pierre Simon Laplace, Paris, France	2.5° × 1.25°
15 MIROC-ESM	Japan Agency for Marine-Earth Science and Technology, Kanagawa, Japan	2.8° × 2.8°
16 MIROC5	Atmosphere and Ocean Research Institute, The University of Tokyo, Chiba, Japan	1.4° × 1.4°
17 MPI-ESM-LR	Max Planck Institute for Meteorology	1.875° × 1.875°
18 MPI-ESM-MR	Max Planck Institute for Meteorology	1.875° × 1.875°
19 MRI-CGCM3	Meteorological Research Institute, Tsukuba, Japan	1.125° × 1.125°
20 NorESM1-M	Norwegian Climate Centre	2.5° × 1.8°

**Fig. 1** Study area located from 5° to 35° longitude and -15° to 15° latitude

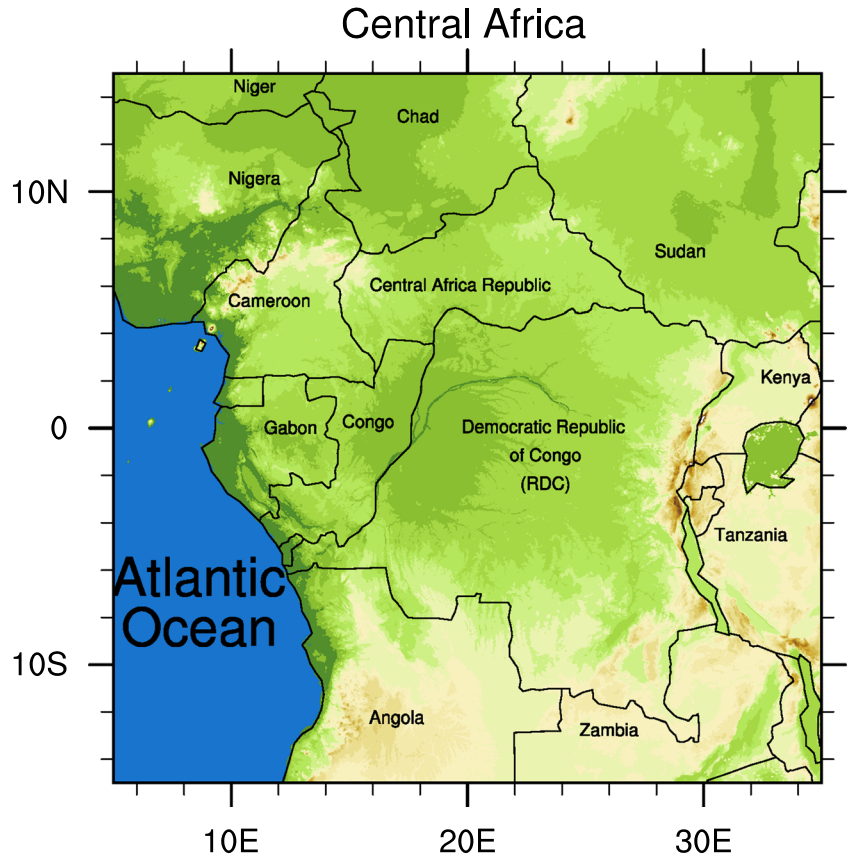


**Table 2** Definitions of the daily rainfall indices used in this study. For each rainfall index, the number of selected high-performing GCMs simulations used to compute the MME according to the Taylor diagram analysis is also reported for every season

Indices ID	Name	Definition	Units	DJF	MAM	JJA	SON
PRCPTOT	Total wet day rainfall	Total rainfall amount in rainy days ( $RR \geq 1$ mm)	mm	11	10	15	08
RR1	Total wet-day rainfall	Number of days with $RR \geq 1$ mm	day	07	12	04	11
SDII	Simple rainfall intensity index	Total wet days rainfall divided by the number of wet days	mm/day	13	02	07	—
RX5DAY	Consecutive 5-day rainfall	Maximum consecutive 5-day rainfall amount	mm	13	03	06	04
CDD	Consecutive dry days	Maximum number of consecutive days with $RR < 1$ mm	day	20	14	18	19
CWD	Consecutive wet days	Maximum number of consecutive days with $RR \geq 1$ mm	day	—	—	—	—
R95	95th percentile	95th percentile of daily rainfall events	mm/day	14	03	05	—
R95PTOT	Total very wet days	Total rainfall amount in rainy days when $RR \geq 95$ th	mm	14	06	11	06

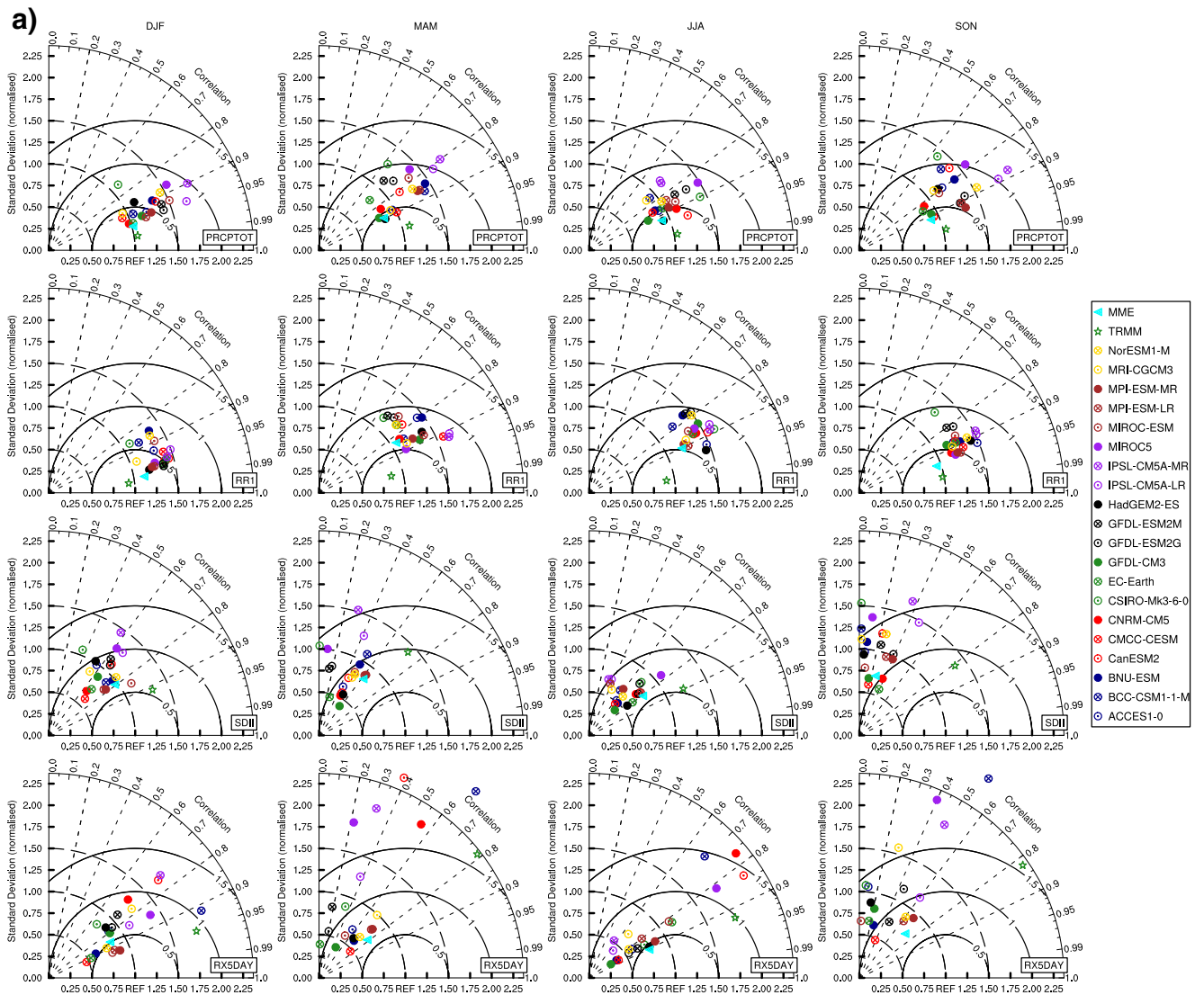


**Fig. 2** Taylor diagram from each of the 20 GCMs simulations, observation dataset TRMM and MME, averaged over the study domain (land grid only). **a** Total wet day rainfall amount (PRCPTOT, first row), wet day frequency (RR1, second row), wet day intensity (SDII, third row), and maximum consecutive 5-day rainfall amount (RX5DAY,

fourth row). **b** Maximum consecutive dry day (CDD, first row), maximum consecutive wet day (CWD, second row), 95th percentile (R95, third row), and total wet day rainfall amount above the 95th percentile (R95PTOT, fourth row). With GPCP considered here as reference dataset

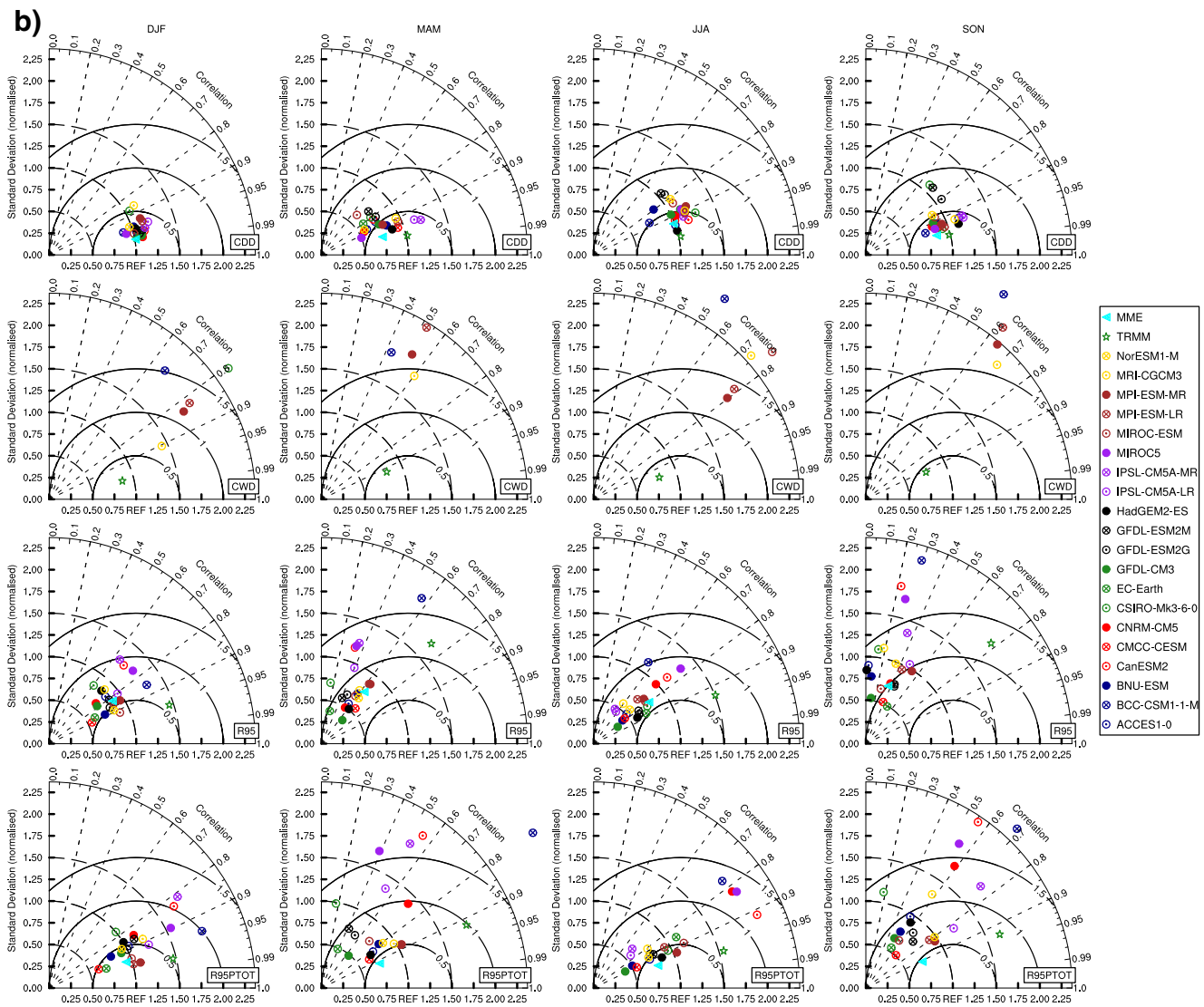


Fig. 2 (continued)

future projection under RCP8.5. For evaluation purposes, simulated rainfall indices are compared to those of two observational datasets which include the following:

- The Global Precipitation Climatology Project 1DD (GPCP version 1.2; Huffman et al. 2009). GPCP is a daily rainfall dataset which the algorithm combines rainfall estimates from several sources including infrared, passive microwave rain estimates, and rain gauge observations. GPCP is available from 1997 to 2014 at a  $1.0^\circ \times 1.0^\circ$  horizontal grid resolution.
- The Tropical Rainfall Measurement Mission 3B42 (TRMM version 7; Huffman et al. 2010). TRMM consists a 3-hourly rainfall database which combines rainfall estimates from various satellite systems as well as feasible land surface rain gauge analysis. TRMM is available for the period spanning from 1998 to 2013 at a  $0.25^\circ \times 0.25^\circ$  horizontal grid resolution.

It is worth mentioning that despite the fact that these two gridded observations may have some uncertainties partly due to the bias in satellite measurement (Nikulin et al. 2012), they have recently shown remarkable performance over Africa where daily rainfall gauge datasets are very scarce (Nikulin et al. 2012; Sylla et al. 2013; Akinsanola et al. 2017). To address uniformity between models and observations, all datasets were interpolated to a common GPCP's horizontal grid ( $1.0^\circ \times 1.0^\circ$ ) over the study area shown in Fig. 1 as follows: All GCMs whose resolution is similar or coarser resolution than  $1.0^\circ$  have been remapped using a bilinear interpolation method; but to keep the original high-resolution information of TRMM which the native resolution is smaller than  $1.0^\circ$ , we used the distance-weighted interpolation method.

In this work, we consider eight daily rainfall indices defined by the Expert Team on Climate Change Detection

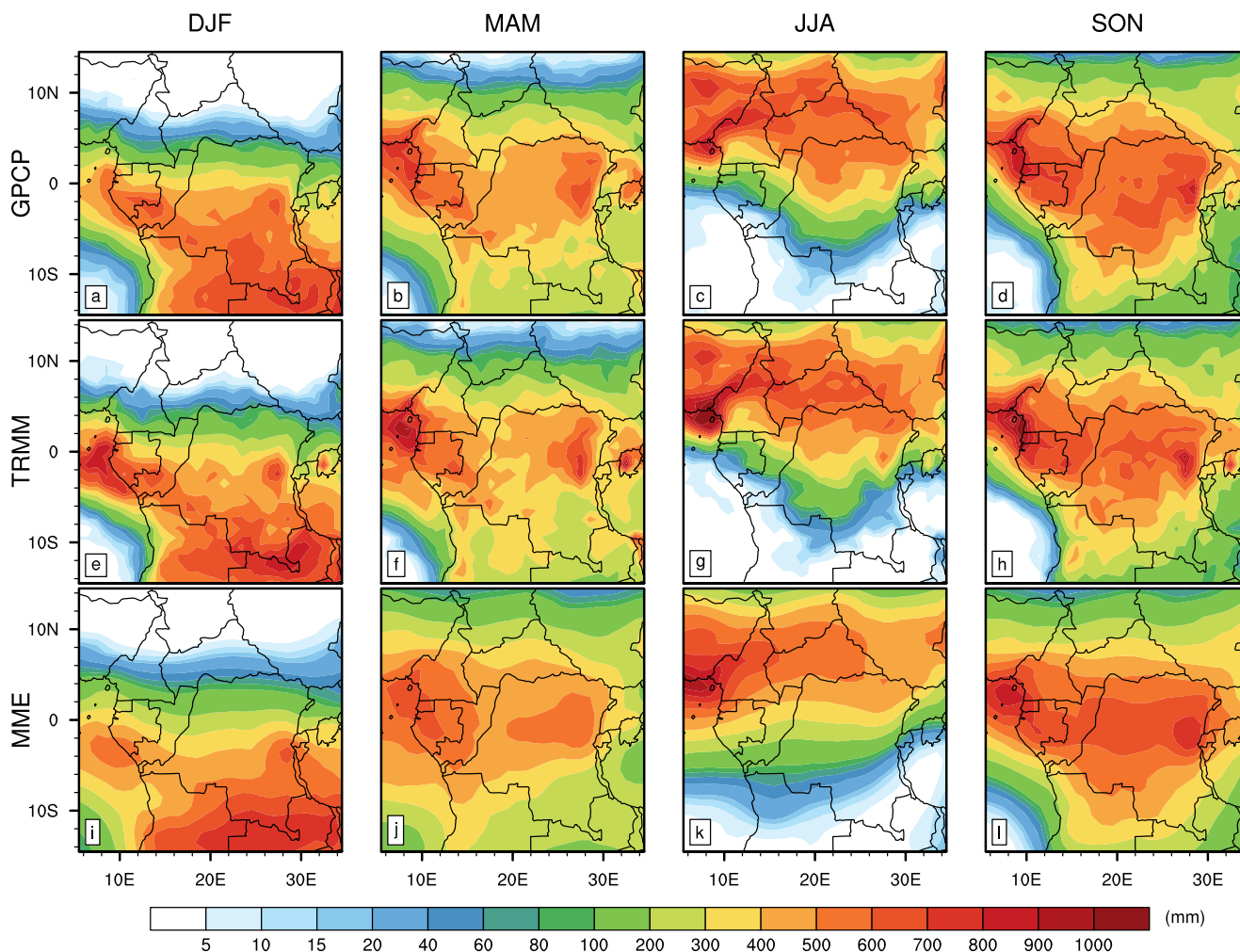


**Fig. 3** Spatial distribution of seasonal total wet day rainfall amount (PRCPTOT, in mm), averaged for the historical period (1998–2005). **a–d** GPCP. **e–h** TRMM. and **i–l** MME

and Indices (ETCCDI; <http://etccdi.pacificclimate.org/>; see Table 2 for detail). These indices have been widely used in the detection, attribution, and projected changes in extreme weather conditions over Africa (e.g., Sylla et al. 2015; Diallo et al. 2016; Abiodun et al. 2017; Nikulin et al. 2018; Pokam et al. 2018a; Akinsanola and Zhou 2018b). Taking into account the seasonal distribution and evolution of different indices used over the whole Central African domain (see, Fig. 1), all the analyses will be made for all seasons, i.e., December-January-February (DJF), March-April-May (MAM), June-July-August (JJA), and September-October-November (SON). For the evaluation of GCMs simulations to reproduce daily rainfall indices over Central Africa during the current period, we have used a common period across models and observations (1998–2005), while for the projected changes, two future 30-year periods are considered: 2026–2055 and 2066–2095 for the mid and late twenty-first century, respectively, with 1976–2005 used as the reference period.

During the historical period, the agreement between the simulated and observed daily rainfall indices is evaluated through the Taylor diagram (Taylor 2001), which provides a concise statistical summary of the degree of correlation (PCC; pattern correlations coefficient), root mean square error (RMSE), and standard deviation (SD). The similarity between simulations and observations is therefore quantified in terms of their correlation and the amplitude of the variability. The highly performing models are selected according to the following two criteria:

- The PCC (i.e., the cosine of the azimuthal angle in a polar coordinate in the figure) should be greater than 0.6;
- The SD (i.e., ratio of standard deviation of simulated and observed fields) should be within the range of  $1.00 \pm 0.25$ .

Note that  $SD > 1$  indicates that simulated values are more variable than those of the observation used as reference.

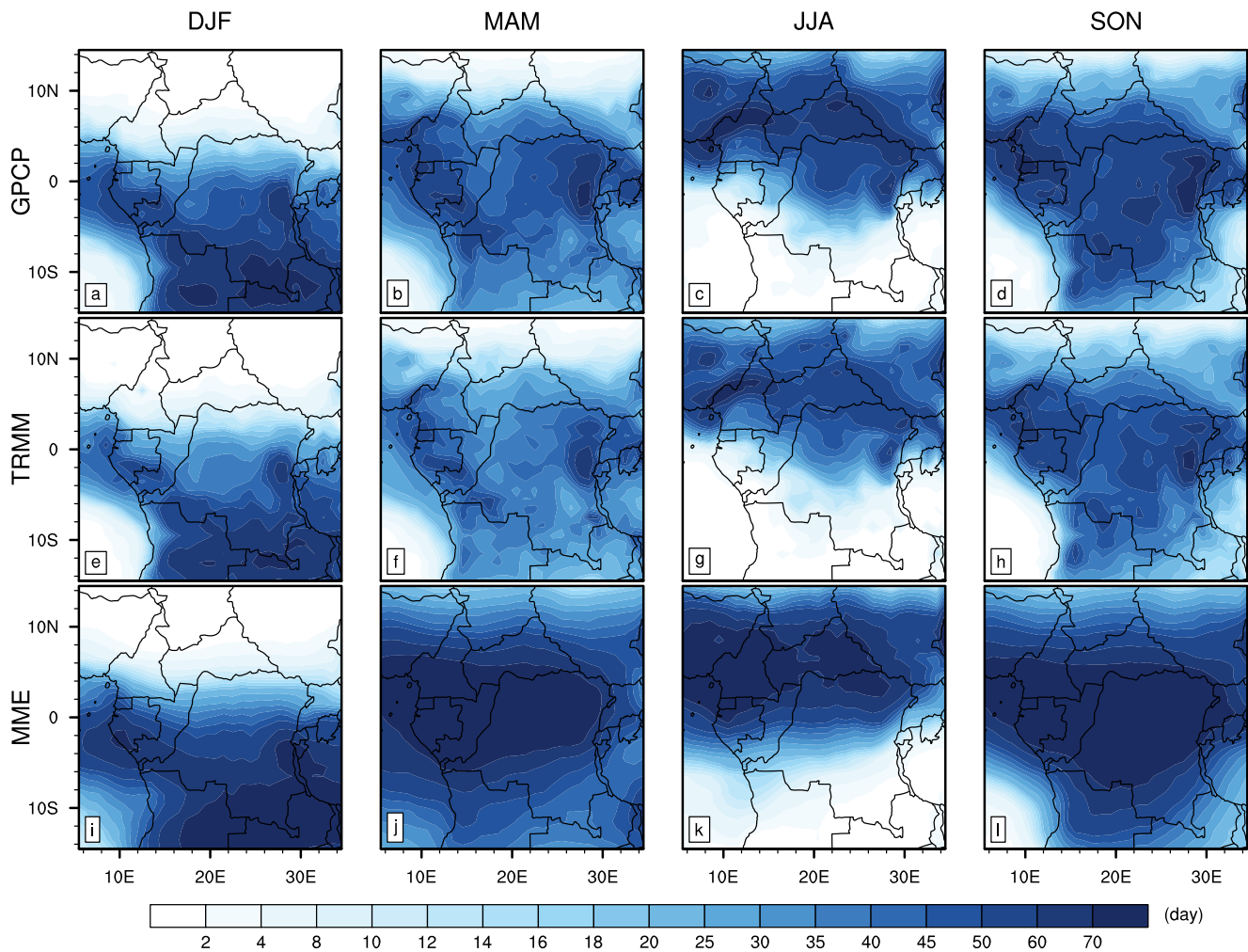


**Fig. 4** Spatial distribution of wet day frequency (RR1, in day), averaged for the historical period (1998–2005). **a–d** GPCP. **e–h** TRMM. and **i–l** MME

During the future period, the significance and robustness of the climate change signal is defined according to the methodologies used in previous studies, in order to measure the model agreement and thus the reduction of uncertainty in the projected changes (Collins et al. 2013; Nikulin et al. 2018). So the climate change signal is robust if the following two criteria are fulfilled:

- More than 80% of GCMs simulations agree on the sign of the change;
- The signal-to-noise ratio (SNR; i.e., the ratio of the mean and the standard deviation of the ensemble of climate change signals is > 1).

### 3 Results and discussion

#### 3.1 Evaluation of daily rainfall indices

We first evaluate the degree of agreement between the simulated and observed rainfall indices (see, Table 2) during

the historical period. Figure 2 presents the seasonal Taylor diagram of different rainfall indices used, averaged over the study domain (land grid only), computed for TRMM, each of the 20 GCMs simulations (see, Table 1), and the multi-model ensemble mean (MME), which here refers to the overall average of models. Since recent studies have shown that GPCP data is more consistent with rain gauge datasets than other gridded observations for the representation of rainfall indices (Sylla et al. 2013; Odoulami and Akinsanola 2017), we choose GPCP as the reference grid point.

The performance of GCMs simulations to reproduce daily rainfall indices shows a wide spread and varies across each index and season. For example, for the case of total wet day rainfall (PRCPTOT; Fig. 2a, first row), all GCMs simulations have a PCC higher than 0.6 in all seasons, but we retained only those which in addition have a SD closer to 1 (i.e., to the reference GPCP). Thus, only the best models selected through this analysis were used to compute the MME for each index (cyan triangle in Fig. 2). In this case, the MME consistently outperforms individual models.

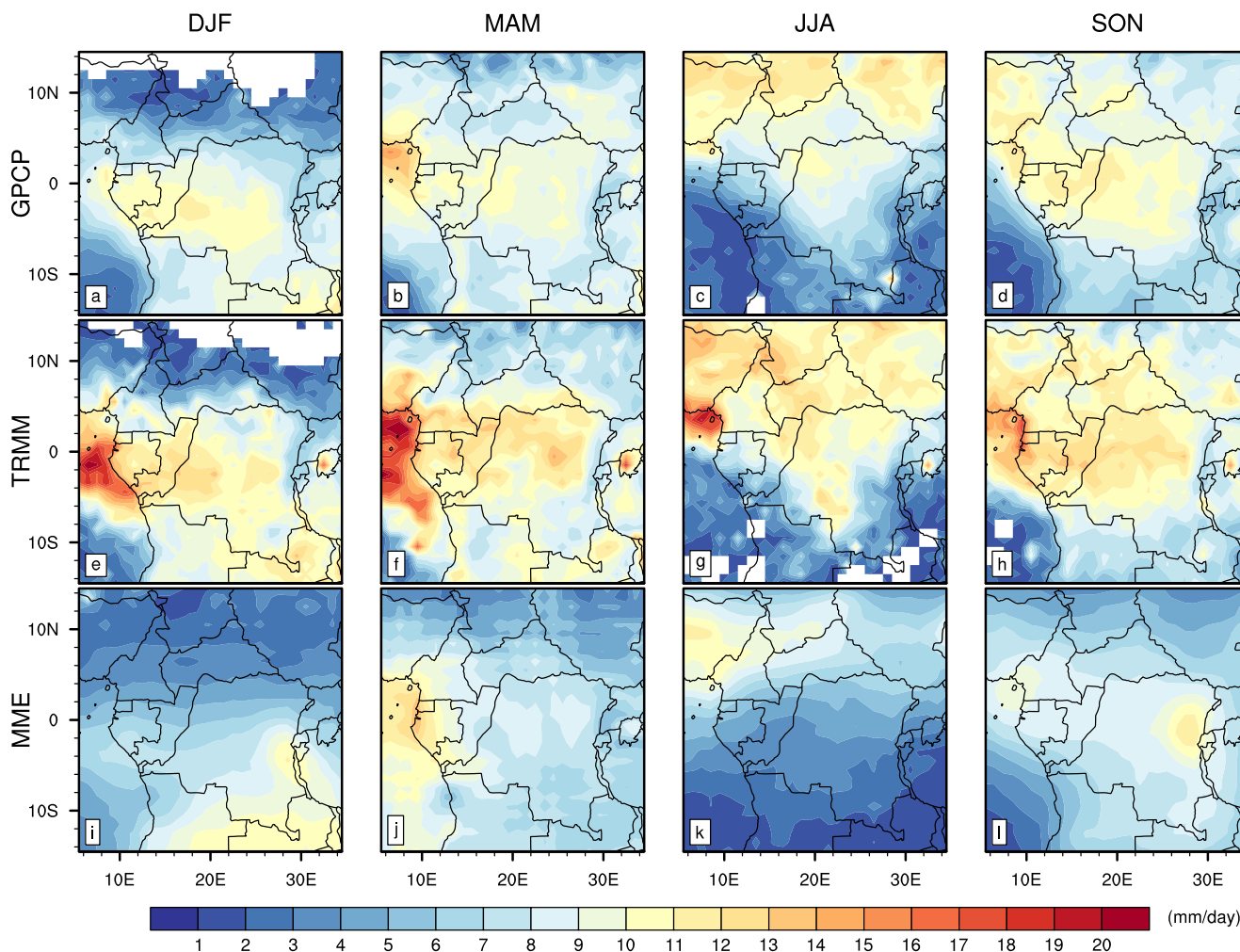


**Fig. 5** Spatial distribution of wet day intensity (SDII, in mm/day), averaged for the historical period (1998–2005). **a–d** GPCP. **e–h** TRMM. and **i–l** MME

This good performance would be linked to a combination of skillful process representation and horizontal resolution of individual members, which has the effect of reducing or cancelling individual model errors (Phillips and Gleckler 2006; Knutti et al. 2010; Aloysius et al. 2016). On the other hand, for the maximum consecutive wet day (CWD; Fig. 2b, second row), some models have PCC greater than 0.6 but all have very large SD, so their dots are sometimes outside the quadrant. This large SD is related to a wet model bias which seems to be intrinsic to the majority of GCMs simulations (also see, Fig. 2a, first row). This result is consistent with that obtain by other authors with GCMs simulations (Bellucci et al. 2010; Li and Xie 2014; Aloysius et al. 2016; Akinsanola and Zhou 2018a). They concluded that the presence of large wet bias exhibited by some GCMs simulations during the rainy season does not necessarily affect their skill in simulating the historical rainfall on the annual scale (Li and Xie 2014; Aloysius et al.

2016). Despite the fact that some models have a relatively high PCC, we did not retain any models because of their SD which is excessively high, consequently degrades the overall skill of the MME (Krishnamurti et al. 2000). In this case where no model meets the Taylor diagram's criteria, and in default to have no data to continue our investigations, we built the MME using all the 20 GCMs simulations. It is also the case in SON for wet day intensity (SDII; Fig. 2a, third row) and 95th percentile of rainfall (R95; Fig. 2b, third row), where it is rather the opposite effect which is observed: the PCC is very small and the SD is in the range  $1.00 \pm 0.5$ . The same approach was used for all indices and the corresponding number of selected high-performing models used to compute the MME for each index and for each season (if any) is recorded in Table 2.

Figure 3 shows the seasonal spatial distribution of PRCPTOT, for observations (GPCP and TRMM) and the



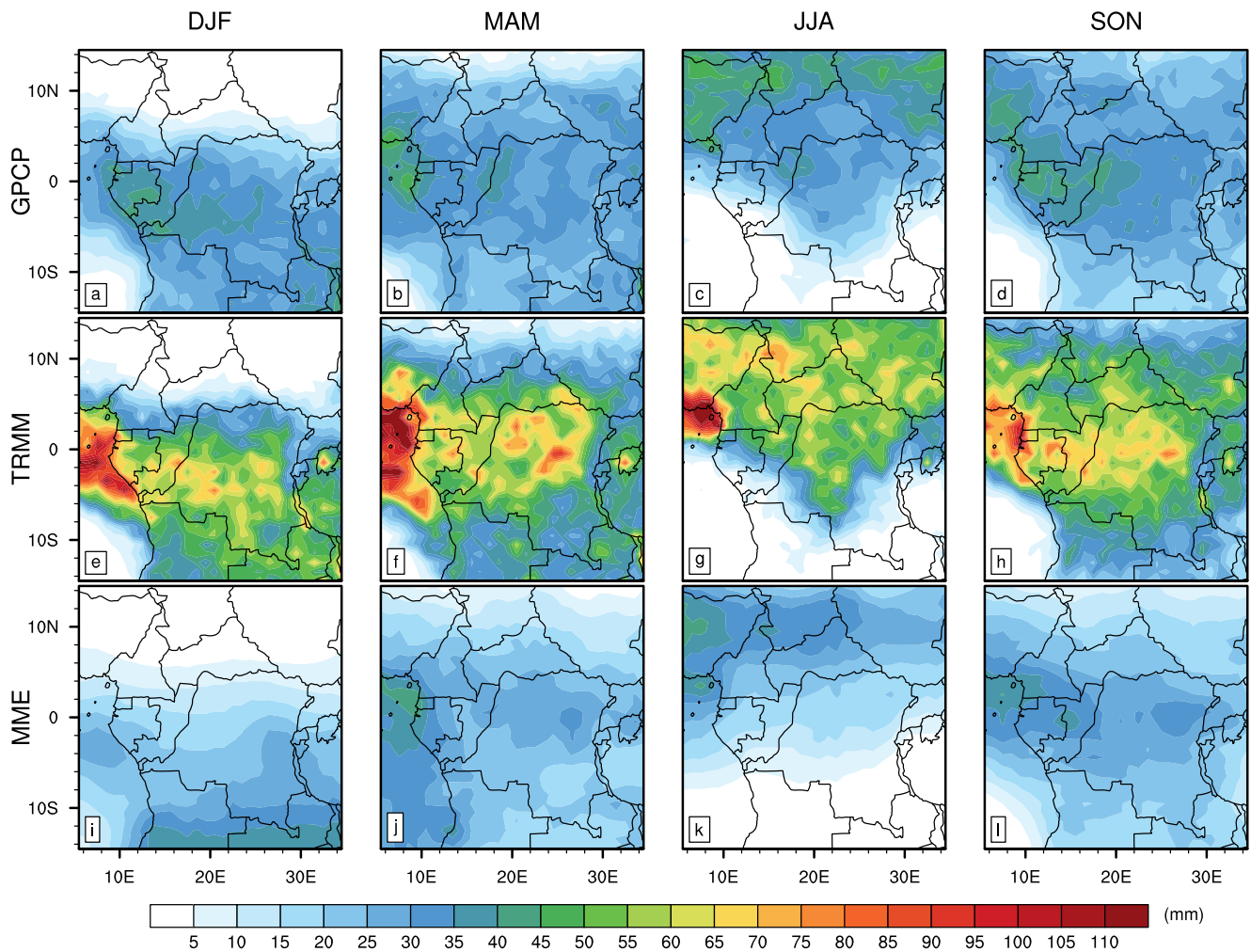


**Fig. 6** Spatial distribution of maximum consecutive 5-day rainfall amount (RX5DAY, in mm), averaged for the historical period (1998–2005). **a–d** GPCP. **e–h** TRMM. and **i–l** MME

MME. During DJF season, GPCP shows the rain-belt in the southern part of the domain between 15° S and 5° N, which decreases gradually from south eastern Central Africa (where the peak of about 1000 mm is observed around eastern Zambia) to the Atlantic Ocean (Fig. 3a). In JJA season, the rain-belt is located between 5° S and 15° N, with a maximum observed over western Cameroon and with a larger extend over northern Central African Republic (Fig. 3c). During MAM and SON seasons, the most part of the domain shows the values of PRCPTOT greater than 100 mm, with the maximum of about 1000 mm along the Guinean Gulf (Fig. 3b, d). It is important to note that in term of rainfall amount, the spatial patterns of PRCPTOT exhibits more rainfall over the region in SON than in MAM. The spatial distribution of PRCPTOT presented by TRMM shows the same patterns as in GPCP, with almost similar patterns and peaks throughout the year (Fig. 3e–h). The PCC between TRMM and GPCP is always greater than 0.9

(green star in Fig. 2a; first row), indicating a good level of agreement between observations for the representation of the total wet day rainfall amount. Compared to the observations, the MME succeeds to simulate the main features of the PRCPTOT’s patterns, with PCC always greater than 0.9 in all seasons, SD closer to 1, and RMSE always smaller than 0.5 (Fig. 2a; first row). Despite the relative good performance of the MME in simulating the total rainfall amount in rainy days, we still note a slight underestimation of this index from March to November (Fig. 2a; first row).

Figures 4 and 5 show the spatial distribution of wet day frequency (RR1) and SDII, respectively, for observations GPCP and TRMM as well as the MME. From one season to another, the observed spatial patterns of RR1 are similar between GPCP and TRMM (Fig. 4a–h). In terms of spatial distribution, these patterns are consistent with those of PRCPTOT shown in Fig. 3, with GPCP always greater

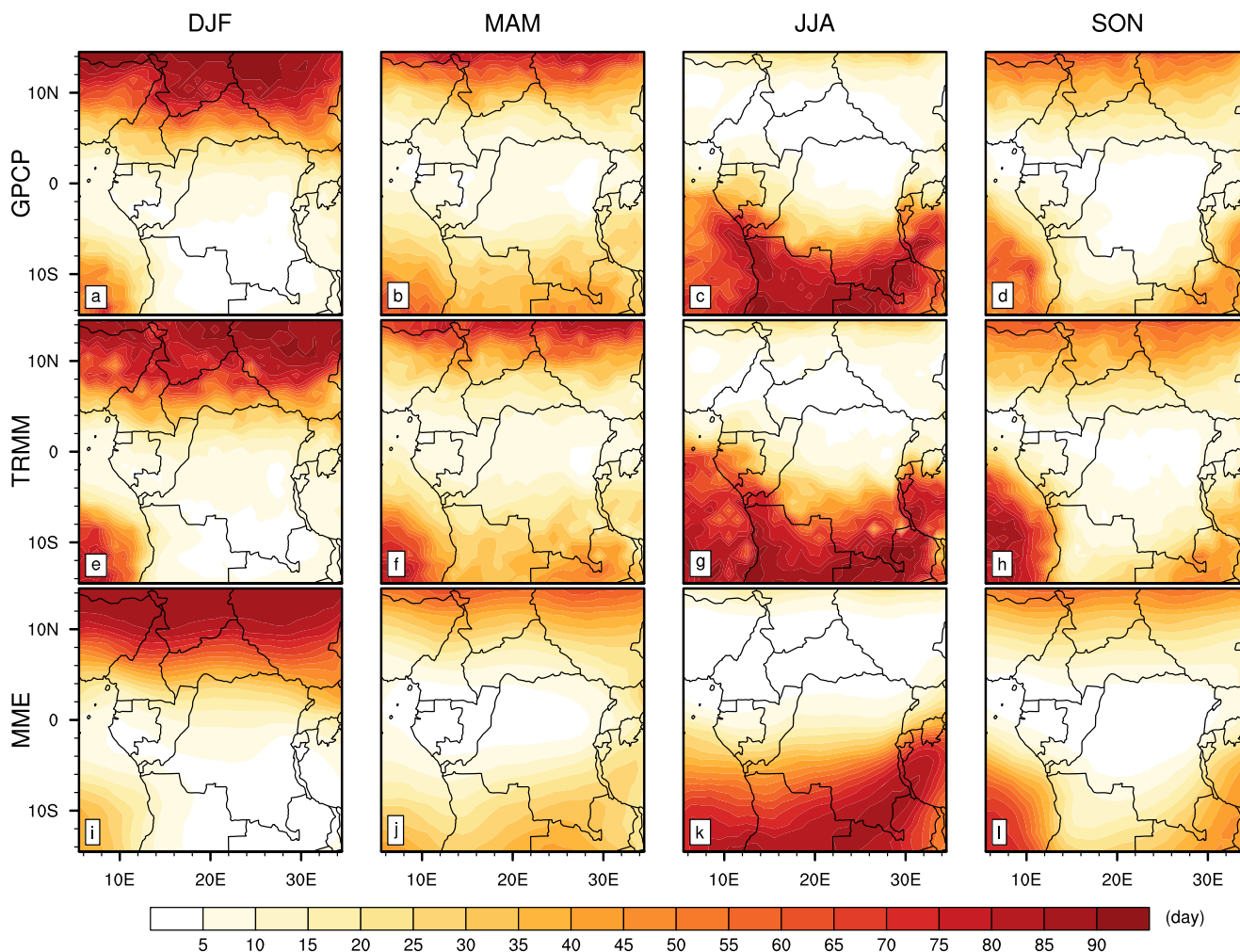


**Fig. 7** Spatial distribution of maximum consecutive dry day (CDD, in day), averaged for the historical period (1998–2005). **a–d** GPCP. **e–h** TRMM. and **i–l** MME

compared to TRMM. This can be observed in the Fig. 2a (second row), with the green star of TRMM always below the reference GPCP. Concerning SDII, the spatial patterns of TRMM are generally greater than 2 mm/day over the region with peaks of up to 18 mm/day which coincide throughout the year with the positions of the maximum of PRCPTOT recorded in Fig. 3a–d. Note that there is some disagreement between GPCP and TRMM especially on less intense events. TRMM appears to be most intense compared to GPCP, and this behavior is in fact associated with its higher spatial resolutions and therefore its high variability (Fotso-Nguemo et al. 2017; Akinsanola and Zhou 2018b). The MME reproduces the overall structure of the seasonal patterns of both RR1 and SDII, but simulates a large occurrence of rainfall events along the rain-belt compared to observations, with PCC always closer to 0.9 in all seasons and RMSE always smaller than 1 (Fig. 2a; second row).

In fact, the MME produces large occurrence of rainfall events (Fig. 2a; second row) and less intense events (Fig. 2a; third row) than observations over the whole Central Africa. So, the neutralization of the contributions of these two indices in the total rainfall amount in rainy days could explain its relative good performance shown in Fig. 2a (first row).

Figure 6 shows the maximum consecutive 5-day rainfall amount (RX5DAY), from both observations GPCP and TRMM as well as the MME. The patterns of RX5DAY exhibited by GPCP and TRMM follows those of SDII shown in Fig. 5. In terms of magnitude, the spatial pattern of TRMM is higher than that of GPCP through all domains, with maximum of up to 100 mm in the Guinean Gulf. As in the case of wet day intensities, the discrepancy among observations for the representation of the maximum consecutive 5-day rainfall amount is linked to

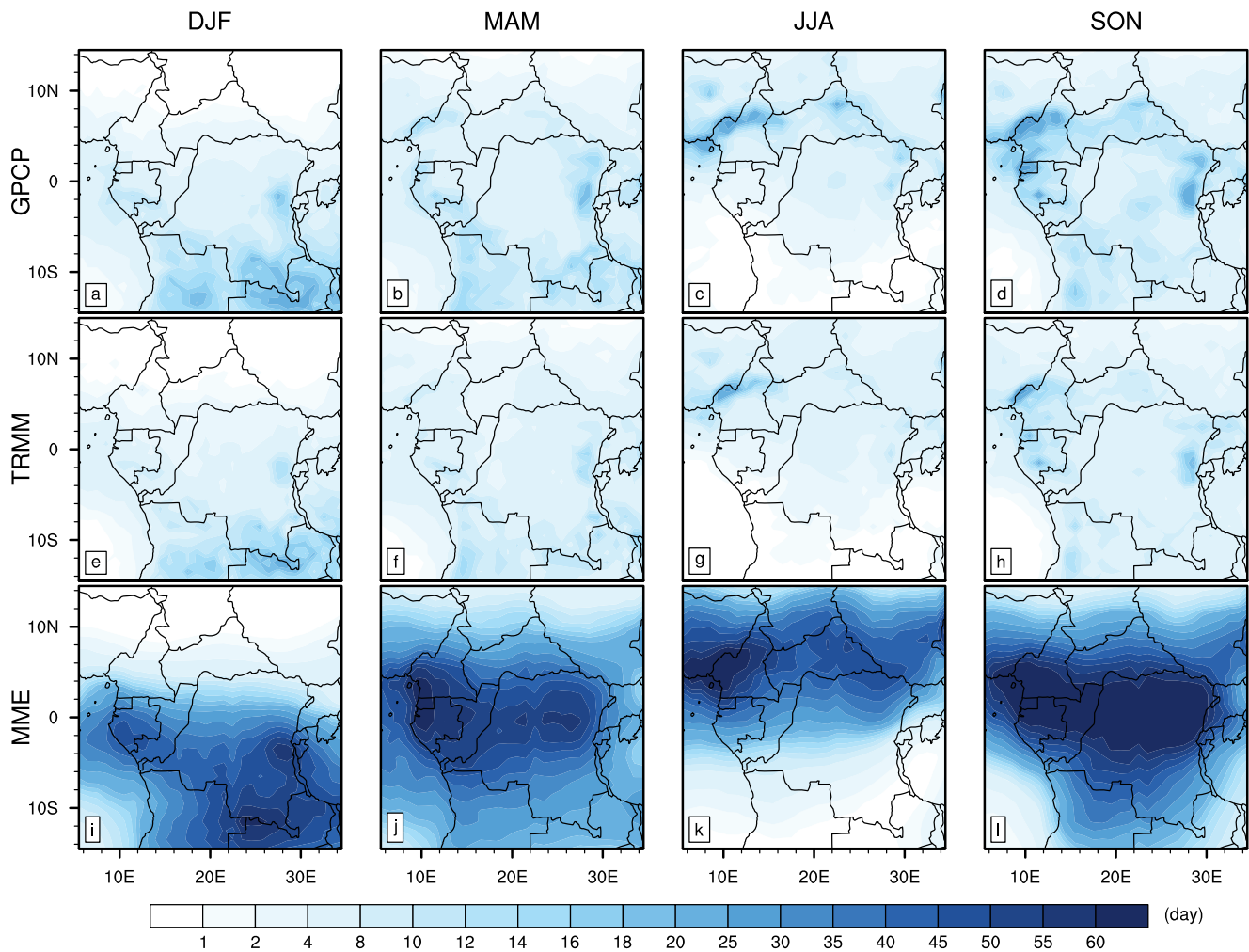


**Fig. 8** Spatial distribution of maximum consecutive wet day (CWD, in day), averaged for the historical period (1998–2005). **a–d** GPCP. **e–h** TRMM. and **i–l** MME

the higher variability of TRMM. Although there are some underestimations compared to GPCP (SD always below 1 in Fig. 2a; fourth row), the MME reproduces the overall structure of the seasonal patterns of RX5DAY (Fig. 6i–l), with PCC always greater than 0.7 in all seasons (Fig. 2a; fourth row).

Figures 7 and 8 show the spatial distribution of the maximum consecutive dry day (CDD) and CWD, respectively, from the MME and observations GPCP and TRMM. The opposite phases in magnitude are well observed between CDD and CWD patterns: areas with minimum CDD correspond to maximum CWD. As expected, the patterns of the lowest CDD are located in areas where PRCPTOT is higher (see, Figs. 3a–h and 7a–h). The MME realistically reproduces the CDD, with PCC always exceeding 0.9 in all seasons, SD closer to 1, and RMSE always smaller than 0.5 (Fig. 2b; first row). But we consistently overestimate the

observed CWD with a very wide SD, so that almost all of the model's dots are outside the diagram (Fig. 2b; second row).

Figures 9 and 10 show the spatial distribution of R95 and total wet day rainfall amount above the 95th percentile (R95PTOT), respectively, from observations GPCP and TRMM as well as the MME. The spatial patterns of R95 follow those of SDII with values of TRMM consistently greater than those of GPCP. Concerning R95PTOT, its spatial pattern is very close to that of PRCPTOT but with maximum rainfall of about 200 mm in all studied seasons. This implies that during all seasons, the recorded rainfall amount is not induced by heavy rainfall events over Central Africa. A similar result was also reported by Sylla et al. (2015) over West Africa. Generally, the MME reproduces the observed spatial pattern field of R95 and R95PTOT, but with lower magnitude.

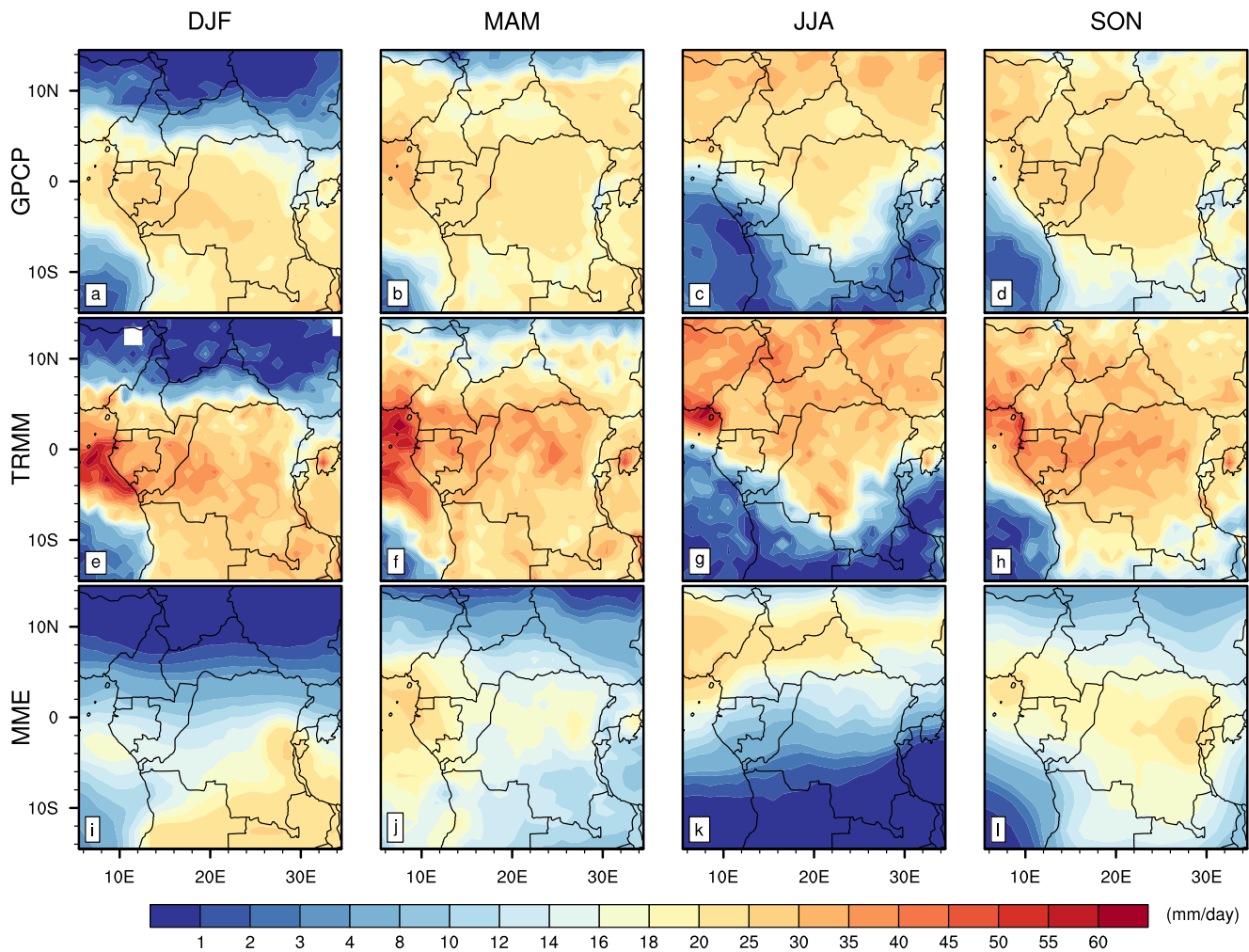


**Fig. 9** Spatial distribution of 95th percentile (R95, in mm/day), averaged for the historical period (1998–2005). **a–d** GPCP. **e–h** TRMM. and **i–l** MME

In summary, the MME captures quite well the observed rainfall indices over the studied domain and is usually found in the range of variability of the considered individual models. This suggests that although there will always exist uncertainty between the models used, the MME of high-performing models obtained from the Taylor diagram analysis can be used in regional climate change assessment (Knutti et al. 2010; Aloysius et al. 2016).

### 3.2 Projected changes of daily rainfall indices

We now turn our attention on the projection of daily rainfall indices under RCP8.5 GHG scenario during the two future 30-year periods (mid and late twenty-first century). Figure 11 shows the spatial distribution of MME seasonal projected change (in %), for PRCPTOT, RR1, SDII, and RX5DAY. The MME projects a significant decrease in PRCPTOT over southern Central Africa in SON with maximum value found around Angola. Recently, Tamoffo et al. (2018) show

that decrease in rainfall and moisture divergence was very correlated across the region, and likely caused by substantial increase of zonal moisture divergence fluxes in upper atmospheric layers. On the other hand, PRCPTOT tends to increase over southern (northern) Central Africa during DJF (SON), with more consistent patterns of change at the late twenty-first century (Fig. 11b; first row). However, there are almost no significant changes during March to August and regions where SNR is  $> 1$  are very small. This indicates that there is a small signal and/or large spread across the GCMs simulations during this period of the year. Differences between mid and late twenty-first century clearly show that PRCPTOT is higher at late twenty-first century and change is more robust compared to mid twenty-first century. For RR1, the MME projects an increase (decrease) which is significant only over certain parts of the study domain during mid twenty-first century (late twenty-first century). Note that the sign of the projected changes almost remains the same for both periods, but the magnitude and area

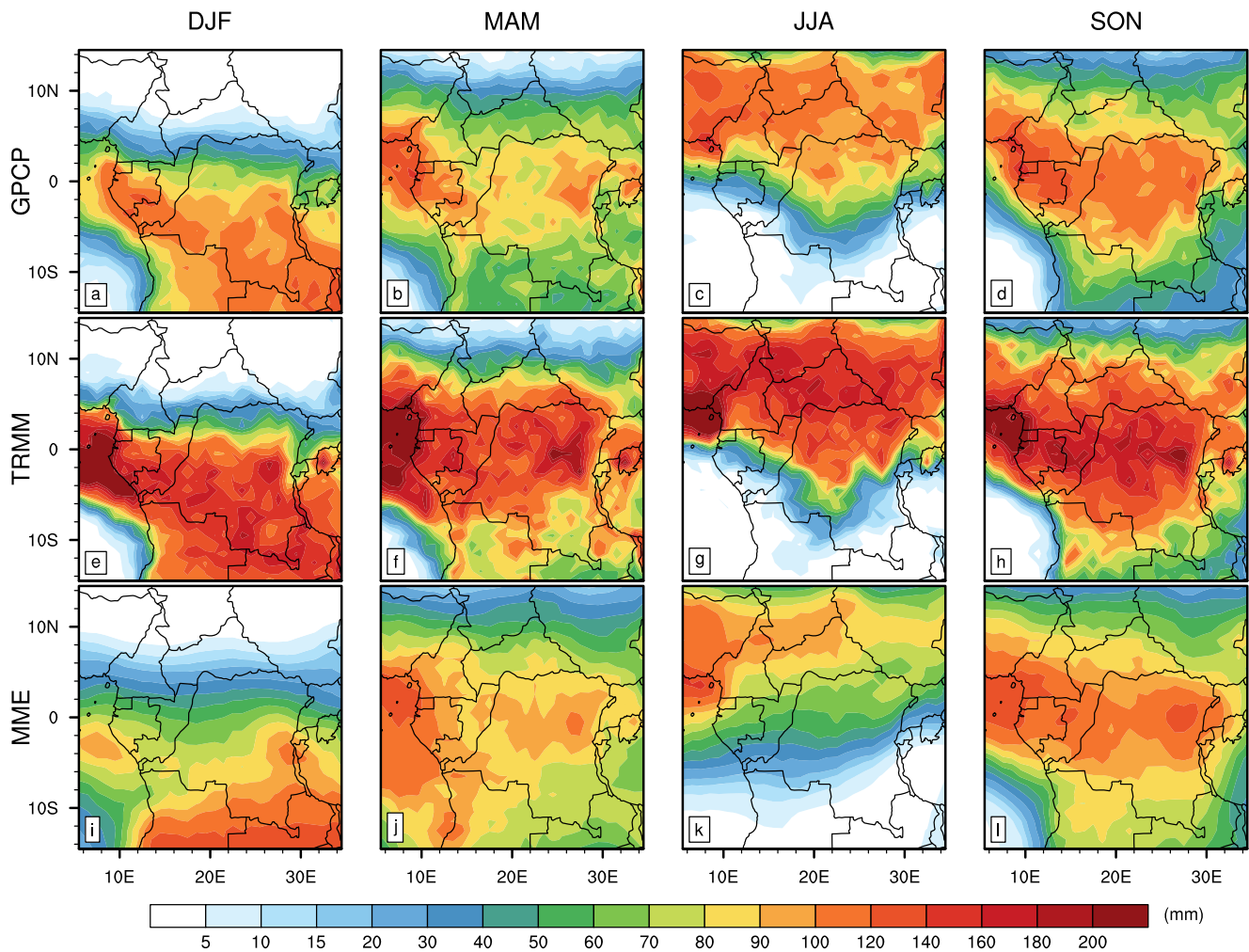


**Fig. 10** Spatial distribution of total wet day rainfall amount above the 95th percentile (R95PTOT, in mm), averaged for the historical period (1998–2005). **a–d** GPCP. **e–h** TRMM. and **i–l** MME

extent of the increase are greater for the mid twenty-first century along Atlantic coast countries (Fig. 11a; second row). The MME for SDII and RX5DAY generally project a consistent increase over the whole Central Africa for both periods, with area of consistent agreement and magnitude larger during late twenty-first century (Fig. 11b; third and fourth rows). A higher SDII means that rainy days become wetter, resulting in more intense rainfall events, even if RR1 decreases. Similar results showing an increase in rainfall intensity through an ensemble of RCMs were also reported over Africa (Déqué et al. 2017; Nikulin et al. 2018). It is possible that the decrease found in PRCPTOT is associated with the decrease in RR1, while its increase is linked to the increase in SDII. This implies that during different seasons, Central Africa will experience strong increase in natural disaster such as flooding mainly due to high intense events, which are more pronounced during the late twenty-first century.

Figure 12 shows the spatial distribution of MME seasonal projected change (in %), for CDD, CWD, R95, and R95PTOT. The projected change patterns of the MME show a significant increase (30–40%) in CDD over southern Central Africa in SON, which is also extended to the Atlantic Ocean from March to November during late twenty-first century (Fig. 12b; first row). The analysis reveals that areas where CDD increases coincide with those where PRCPTOT decreases. The increase in CDD accompanied with the decrease in PRCPTOT could have strong consequences for seasonal rainfall onset in this region, which can impact the rain-fed agriculture, hydroelectric power generation, and water resources management. The increase/decrease becomes weaker at mid twenty-first century, but there is almost no region that agrees with the signal of change, and in most cases, we have the SNR which is  $< 1$  (Fig. 12a; first row). Projected changes in CWD show a significant

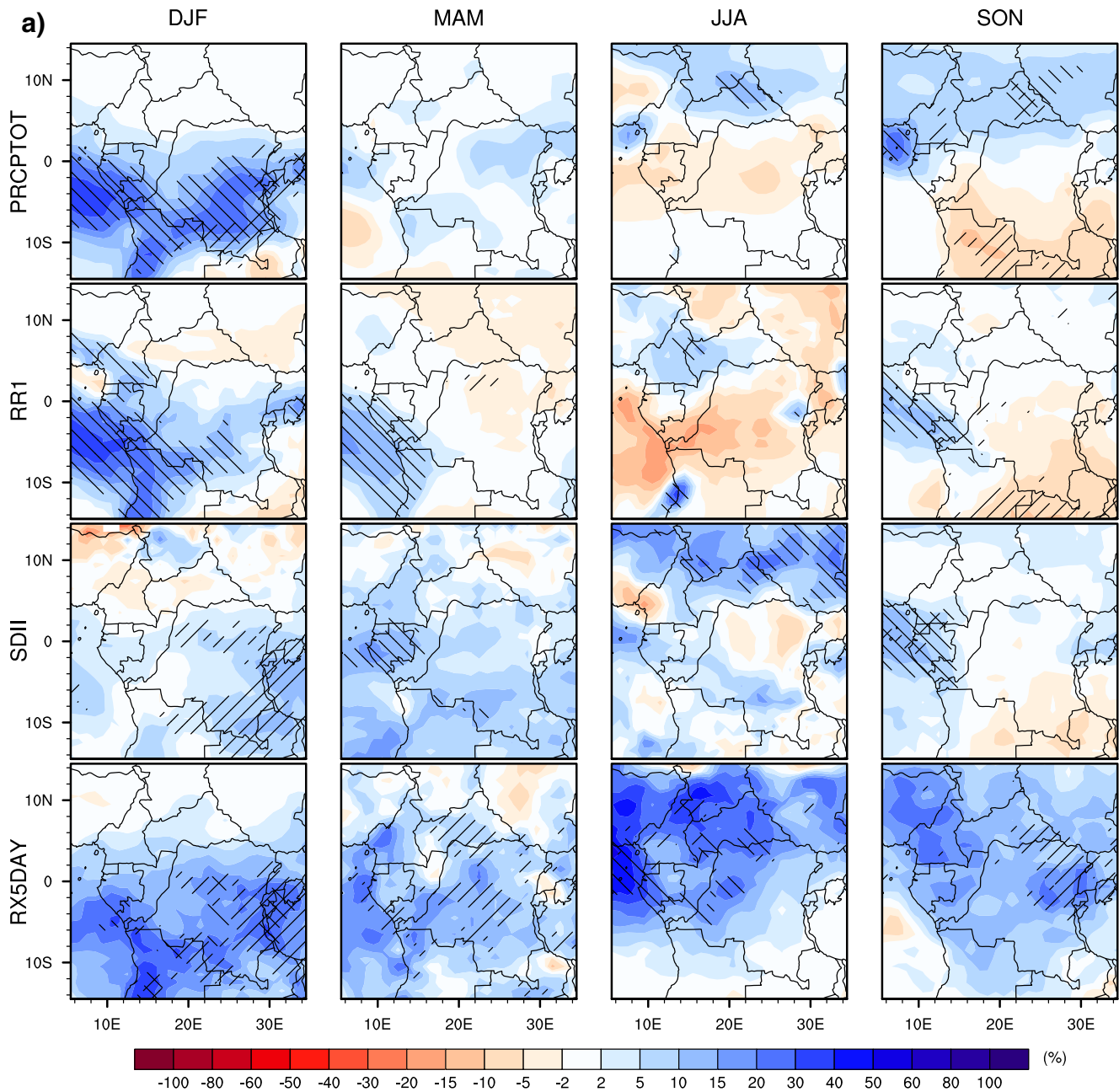


**Fig. 11** Spatial distribution of MME seasonal projected change (in %) between the future and the historical periods. **a** Mid-twenty-first century (2026–2055 minus 1976–2005). **b** Late twenty-first century (2066–2095 minus 1976–2005). For total wet day rainfall amount (PRCPTOT, *first row*), wet day frequency (RR1, *second row*), wet day intensity (SDII, *third row*), and maximum consecutive 5-day rainfall

amount (RX5DAY, *fourth row*), areas where the change is significant (i.e., where least 80 % of simulations agree on the sign of the change) are highlighted by positively sloped hatching ('/'). Areas where the change is robust (i.e., where the SNR is > 1) are highlighted by negatively sloped hatching ('\')

decrease over the majority of the Central African domain during late twenty-first century (Fig. 12b; second row). On contrary, a consistent increase (2–5%) is recorded in DJF over southern Sudan, northern Democratic Republic of Congo, and Kenya. Concerning the mid twenty-first century, the sign of the projected changes remains the same

in most part of the domain, although there is almost no agreement on the decrease (Fig. 12a; second row). Projected changes in the R95 and R95PTOT patterns generally show a consistent increase over most part of the domain for both mid and late twenty-first century. Projected patterns of R95 and R95PTOT are more robust for late twenty-first

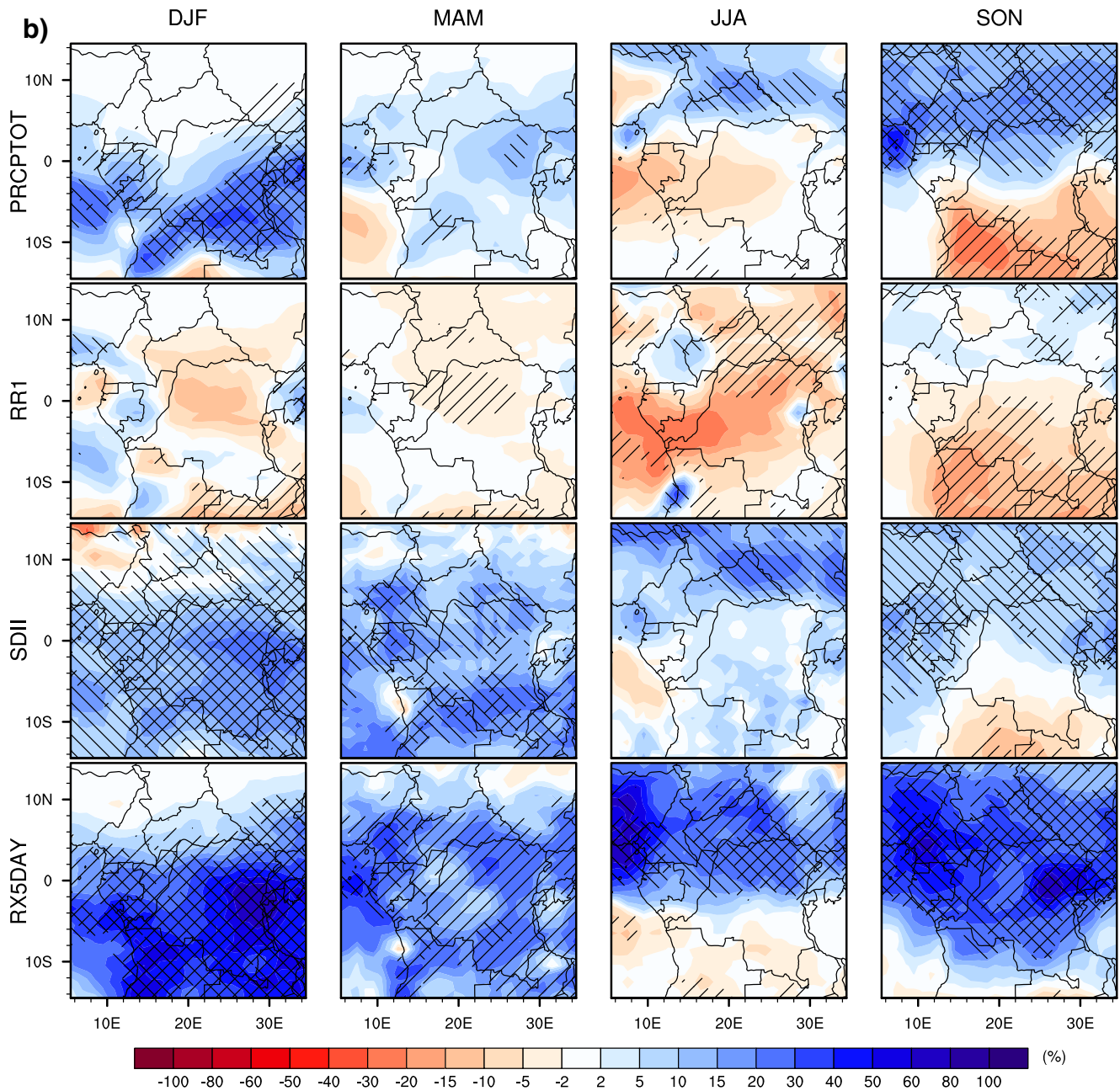
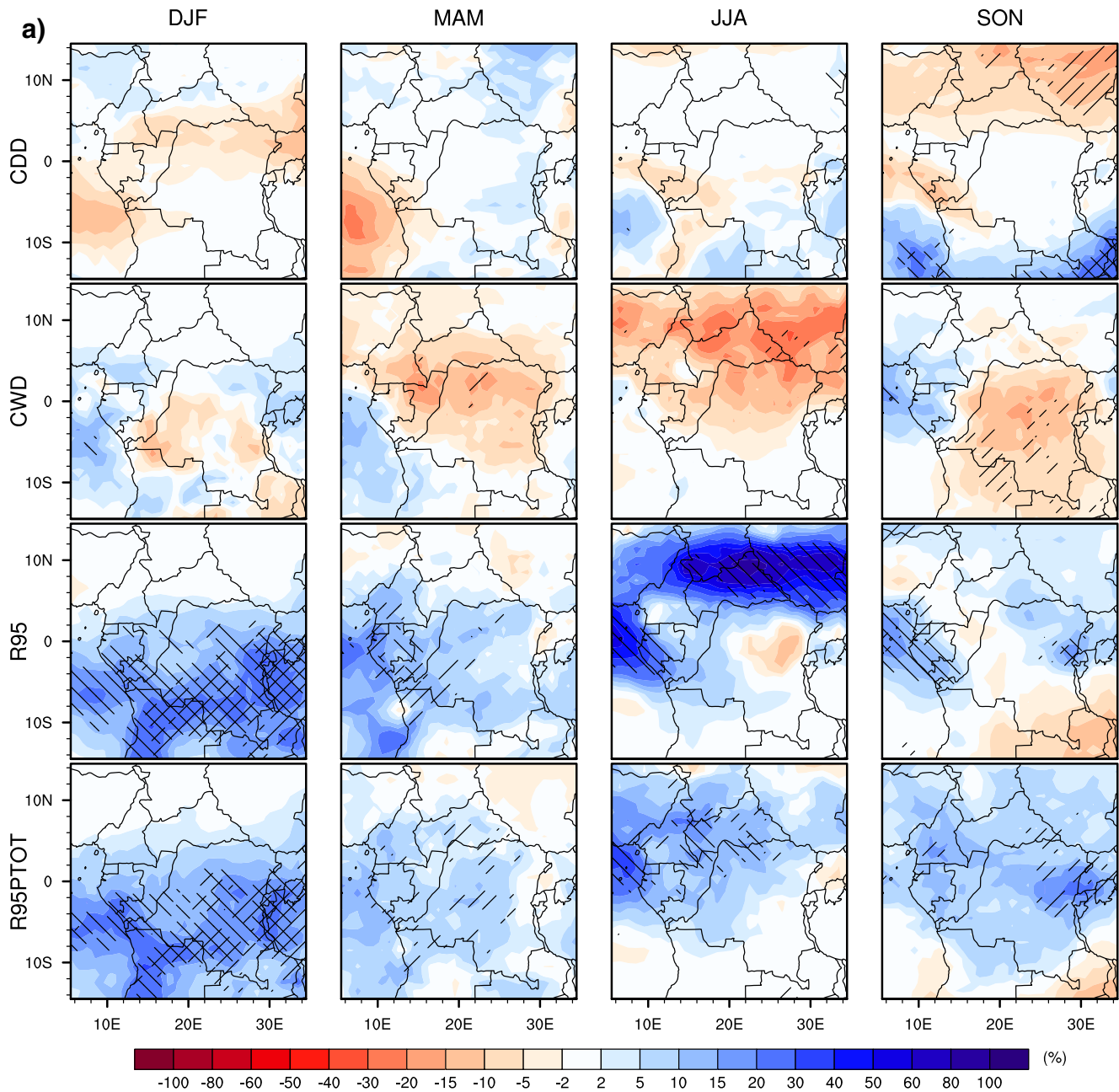


Fig. 11 (continued)

century than those for mid twenty-first century. The increase in both R95 and R95PTOT means that extreme rainfall events could be more intense in the future, which can be associated with the increase of moisture convergence intensified by the presence of the Congo Basin rain forest (Dyer et al. 2017; Fotso-Nguemo et al. 2018) and is likely to multiply the probability of flood risks. Recently, Akinsanola and Zhou (2018a) analyzed the West African summer monsoon rainfall through an ensemble of GCMs simulations, and they found that the increasing rainfall was connected to the increase in surface evaporation and

enhanced atmospheric moisture convergence. However, a significant decrease which coincides with the decrease in PRCPTOT and RR1 is projected in SON over Angola, Zambia, and southern Democratic Republic of Congo. The decrease in both extreme indices R95 and R95PTOT, coupled with a decrease in both PRCPTOT and RR1, implies that in the future, these countries will be subject to high drought risk. Such situation can threaten the water resources availability and therefore affect the food security, which can contribute to increase social riots (Almer et al. 2017).



**Fig. 12** Spatial distribution of maximum consecutive dry day (CDD, *first row*), maximum consecutive wet day (CWD, *second row*), 95th percentile (R95, *third row*), and total wet day rainfall amount above the 95th percentile (R95PTOT, *fourth row*)

Overall, our results obtained through the MME projections indicate that most of Central African countries will experienced a general increase of extreme rainfall events more pronounced during late twenty-first century. The tendency towards increase of extreme rainfall events found in this study is consistent with the main findings in the literature done based on climate models. For instance, the decrease in heavy rainfall noted by Aguilar et al. (2009) over western Central Africa was not found in our analysis. This

can be explained by the fact that the climate change signal of heavy rainfall events found in this study during mid twenty-first century, which is closer to the period used in Aguilar's investigations, was not robust and therefore inconclusive. Our results thus highlight the need to include uncertainties when dealing with the assessment of climate change signal over the region from an ensemble of several models (Knutti et al. 2010; Aloysius and Saiers 2017; Pokam et al. 2018a; Nikulin et al. 2018; Akinsanola and Zhou 2018b).



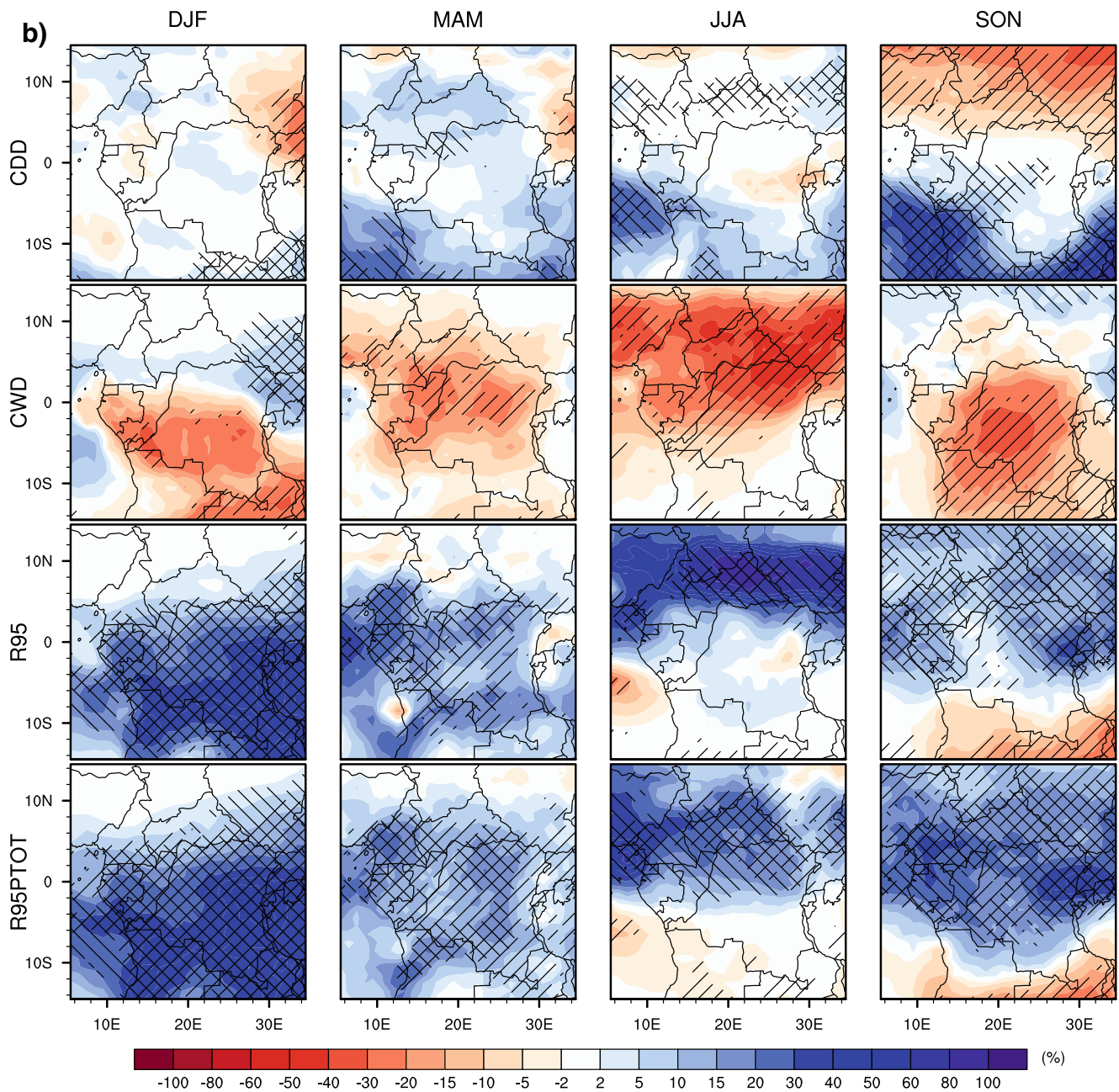


Fig. 12 (continued)

### 4 Summary and conclusions

This study attempts to evaluate the ability of a MME, built on the basis of a selection made among 20 available GCMs simulations participating in the CMIP5 project, to capture the spatial patterns of eight daily rainfall indices over Central Africa, and assess the potential impact of climate change on these indices across the region. For this purpose, the MME has been evaluated during the historical period (1998–2005) in comparison to GPCP and TRMM gridded observation datasets. The future changes in the

eight rainfall indices were assessed by comparing the two future 30-year periods (mid and late twenty-first century; 2026–2056 and 2066–2095 respectively) with the historical time period (1976–2005), under the GHG emission scenario RCP8.5. The MME consists to the ensemble mean of highly performing models selected through the Taylor diagram analysis, which allow to evaluate the degree of agreement between the simulated and observed rainfall indices.

Results show that the two observational datasets, GPCP and TRMM, exhibit substantial differences, with reasonable

agreement for the majority of rainfall indices. This therefore highlights the existence of uncertainties that exist between gridded observations (Nikulin et al. 2012; Sylla et al. 2013; Akinsanola et al. 2017). By taking into account these uncertainties and although the large inter-annual variability shown by some GCMs simulations, we found that the MME consistently outperforms individual models in simulating the climatology of different rainfall indices over Central Africa. Except in the case of CWD where the high variability of individual members has resulted in the degradation of the overall skill of the MME. Given the relative good performance of the MME which could be associated with a combination of skillful process representation and horizontal resolution of individual members (Aloysius et al. 2016), the different MME obtained with each rainfall index can be used in regional climate change assessment (Knutti et al. 2010; Aloysius et al. 2016).

Future changes in daily rainfall indices based the MME projections indicate statistically significant decreases of about 5–15% in PRCPTOT over southern Central Africa in SON, but also an increase of about 10–20% is recorded over southern (northern) Central Africa during DJF (SON), with more agreement patterns of change at late twenty-first century. A significant decrease of about 5–15% in CWD coupled with increase of about 30–40% in CDD is generally observed over Angola, Zambia, and southern Democratic Republic of Congo in SON. These countries are likely to be particularly affected by the negative effects of climate change, not only by the intensification of dry conditions represented by the coupled projected increase (decrease) of CDD (CWD) in SON, but also the intensification of wet conditions which will occur in DJF as predicted by increase in RX5DAY, R95, and R95PTOT. In fact, RX5DAY, R95, and R95PTOT are projected to consistently increase across the studied domain, with most area of agreement in DJF and SON. Recently, other authors have reported that despite the expected moderate projected decrease in the mean rainfall over West Africa, extreme rainfall will considerably increase (Kitoh et al. 2013; Akinsanola and Zhou 2018b). For instance, we can notice that the increase in RX5DAY, R95, and R95PTOT is likely to multiply the probability of flood risks over Gabon, Congo, Angola, Zambia, and Democratic Republic of Congo in DJF, and also over Cameroon, Central African Republic, and northern Democratic Republic of Congo in SON. The consistent and high inter-model agreement on the sign of the change further affirms the reliability of the projected changes, although noticeable uncertainty between models still exists. Furthermore, the magnitudes of the projected increases or decreases are greater during late twenty-first century compared to mid twenty-first century, which may be a result of their different GHG concentration rate sensitivities and their associated feedback mechanisms.

The higher probability of projected natural disasters may threaten the available water resources and thus affect the availability of the food supply, which can increase water scarcity and social riots over Central Africa (Almer et al. 2017). Therefore, it is crucial for the Central African countries, especially those cited in this study, to seriously consider implementing adaptation strategies and mitigation measures to avoid the potential impact of climate change on future rainfall and associated extremes. This study focuses the assessment and the projected change in daily rainfall characteristics over Central Africa and does not touch more complex aspects of the region's climate as for example the onset, cessation, and length of the rainy season which are indeed important. These daily rainfall characteristics will be the subject of our future investigations.

**Acknowledgements** The authors would like to thank the climate modeling groups listed in Table 1, for producing and making available their model output through the website <https://climate4impact.eu/impactportal/data/esgfsearch.jsp>. The Global Precipitation Climatology Project and the Tropical Rainfall Measurement Mission are also acknowledged for providing the gridded datasets used in this study. We gratefully acknowledge the efforts of the two anonymous reviewers whose comments and suggestions substantially improved the first version of the manuscript.

**Publisher's Note** Springer Nature remains neutral with regard to jurisdictional claims in published maps and institutional affiliations.


## References

- Abiodun BJ, Adegoke J, Abatan AA, Ibe CA, Egbebiyi TS, Engelbrecht F, Pinto I (2017) Potential impacts of climate change on extreme precipitation over four African coastal cities. *Climatic Change* 143:399–413. <https://doi.org/10.1007/s10584-017-2001-5>
- Aguilar E, Barry AA, Brunet M, Ekang L, Fernandes A, Massoukina M, Mbah J, Mhanda A, do Nascimento D, Peterson T, Umba OT, Tomou M, Zhang X (2009) Changes in temperature and precipitation extremes in western central Africa, Guinea Conakry, and Zimbabwe, 1955–2006. *J Geophys Res Atmos* 114:D02,115. <https://doi.org/10.1029/2008JD011010>
- Akinsanola AA, Zhou W (2018a) Ensemble-based CMIP5 simulations of West African summer monsoon rainfall: current climate and future changes. *Theor Appl Climatol*, pp 1–11. <https://doi.org/10.1007/s00704-018-2516-3>
- Akinsanola AA, Zhou W (2018b) Projections of West African summer monsoon rainfall extremes from two CORDEX models. *Clim Dyn*, pp 1–12. <https://doi.org/10.1007/s00382-018-4238-8>
- Akinsanola AA, Ogunjobi KO, Ajayi V, Adefisan EA, Omotosho JA, Sanogo S (2017) Comparison of five gridded precipitation products at climatological scales over West Africa. *Meteorol Atmos Phys* 129:669–689. <https://doi.org/10.1007/s00703-016-0493-6>
- Almer C, Laurent-Lucchetti J, Oechslin M (2017) Water scarcity and rioting: disaggregated evidence from Sub-Saharan Africa. *J Environ Econ Manag* 86:193–209. <https://doi.org/10.1016/j.jeem.2017.06.002>
- Aloysius NR, Saiers JE (2017) Simulated hydrologic response to projected changes in precipitation and temperature in the Congo River basin. *Hydrol Earth Syst Sci* 21:4115–4130. <https://doi.org/10.5194/hess-21-4115-2017>

- Aloysius NR, Sheffield J, Saiers JE, Li H, Wood EF (2016) Evaluation of historical and future simulations of precipitation and temperature in central Africa from CMIP5 climate models. *J Geophys Res Atmos* 121:130–152. <https://doi.org/10.1002/2015JD023656>
- Alsford D, Beighley E, Laraque A, Lee H, Tshimanga R, O'Loughlin F, Mahé G, Dinga B, Moukandi G, Spencer RGM (2016) Simulated hydrologic response to projected changes in precipitation and temperature in the Congo River basin. *Hydrol Earth Syst Sci* 21:4115–4130. <https://doi.org/10.5194/hess-21-4115-2017>
- Bellucci A, Gualdi S, Navarra A (2010) The double-ITCZ syndrome in coupled general circulation models: the role of large-scale vertical circulation regimes. *J Clim* 23:1127–1145. <https://doi.org/10.1175/2009JCLI3002.1>
- Chamani R, Monkam D, Djomou ZY (2018) Analysis of return periods and return levels of yearly July–September extreme droughts in the West African Sahel. *Clim Dyn*, pp 1–13. <https://doi.org/10.1007/s00382-018-4336-7>
- Collins M, Knutti R, Arblaster J, Dufresne JL, Fichefet T, Friedlingstein P, Gao X, Gutowski W, Johns T, Krinner G, Shongwe M, Tebaldi C, Weaver A, Wehner M (2013) Long-term climate change: projections, commitments and irreversibility. In: Stocker TF, Qin D, Plattner G-K, Tignor M., Allen SK, Boschung J, Nauels A, Xia Y, Bex V, Midgley PM (eds) *Climate change 2013: the physical science basis. Contribution of working group I to the fifth assessment report of the intergovernmental panel on climate change*. Cambridge University Press, Cambridge. United Kingdom and New York, NY, USA
- Déqué M, Calmanti S, Christensen OB, Aquila AD, Maule CF, Haensler A, Nikulin G, Teichmann C (2017) A multi-model climate response over tropical Africa at +2°C. *Clim Serv* 7:87–95. <https://doi.org/10.1016/j.cliser.2016.06.002>
- Diallo I, Giorgi F, Deme A, Tall M, Mariotti L, Gaye AT (2016) Projected changes of summer monsoon extremes and hydroclimatic regimes over West Africa for the twenty-first century. *Clim Dyn* 47:3931–3954. <https://doi.org/10.1007/s00382-016-3052-4>
- Dyer ELE, Jones DBA, Nusbaumer J, Li H, Collins O, Vettoretti G, Noone D (2017) Congo Basin precipitation: assessing seasonality, regional interactions, and sources of moisture. *J Geophys Res Atmos* 122:6882–6898. <https://doi.org/10.1002/2016JD026240>
- FAO (2018). FAO in emergencies. <http://www.fao.org/emergencies/regions/east-and-central-africa/en/>, (accessed 14 November 2018)
- Fauchereau N, Trzaska S, Rouault M, Richard Y (2003) Rainfall variability and changes in southern africa during the 20th century in the global warming context. *Nat Hazards* 29:139–154
- Fotso-Nguemo TC, Vondou DA, Pokam WM, Djomou ZY, Diallo I, Haensler A, Tchotchou LAD, Kamsu-Tamo PH, Gaye AT, Tchawoua C (2017) On the added value of the regional climate model REMO in the assessment of climate change signal over Central Africa. *Clim Dyn* 49:3813–3838. <https://doi.org/10.1007/s00382-017-3547-7>
- Fotso-Nguemo TC, Chamani R, Yepdo ZD, Sonkoué D, Matsaguim CN, Vondou DA, Tanessong RS (2018) Projected trends of extreme rainfall events from CMIP5 models over Central Africa. *Atmos Sci Lett* 19:1–8. <https://doi.org/10.1002/asl.803>
- Haensler A, Saeed F, Jacob D (2013) Assessing the robustness of projected precipitation changes over central Africa on the basis of a multitude of global and regional climate projections. *Clim Change* 121:349–363. <https://doi.org/10.1007/s10584-013-0863-8>
- Huffman GJ, Adler RF, David TB, Guojun G (2009) Improving the global precipitation record: GPCP Version 2.1. *Geophys Res Lett* 36(L17):808. <https://doi.org/10.1029/2009GL040000>
- Huffman GJ, Adler RF, Bolvin DT, Nelkin EJ (2010) The TRMM Multi-satellite Precipitation Analysis (TMPA). In: Hossain F, Gebremichael M (eds) *Satellite applications for surface hydrology*. Springer, Berlin, pp 3–22. ISBN: 978-90-481-2914-0
- IPCC (2013) Summary for policymakers. In: *Climate change 2013: The physical science basis contribution of working group I to the fifth assessment report of the intergovernmental panel on climate change*. Cambridge University Press, Cambridge. United Kingdom and New York, NY, USA
- Kitoh A, Endo H, Kumar KK, Cavalcanti IF, Goswami P, Zhou T (2013) Monsoons in a changing world: a regional perspective in a global context. *J Geophys Res Atmos* 118:3053–3065. <https://doi.org/10.1002/jgrd.50258>
- Knutti R, Furrer R, Tebaldi C, Cermak J, Meehl GA (2010) Challenges in combining projections from multiple climate models. *J Clim* 23:2739–2758
- Krishnamurti TN, Kishtawal CM, Zhang Z, Larow T, Bachiochi D, Willford E (2000) Multimodel ensemble forecasts for weather and seasonal climate. *J Climate* 13:4196–4216
- Kruger A (2006) Observed trends in daily precipitation indices in South Africa: 1910–2004. *Int J Climatol* 26:2275–2285
- Li G, Xie S (2014) Tropical biases in CMIP5 multimodel ensemble: the excessive equatorial Pacific cold tongue and double ITCZ problems. *J Clim* 27:1765–1780
- Libanda B, Ngonga C (2018) Projection of frequency and intensity of extreme precipitation in Zambia: a CMIP5 study. *Clim Res* 76:59–72
- Nikulin G, Jones C, Samuelsson P, Giorgi F, Asrar G, Büchner M, Cerezo-Mota R, Christensen OB, Déqué M, Fernandez J, Hänsler A, van Meijgaard E, Sylla MB, Sushama L (2012) Precipitation climatology in an ensemble of CORDEX-africa regional climate simulations. *J Clim* 25:6057–6078. <https://doi.org/10.1175/JCLI-D-11-00375.1>
- Nikulin G, Lennard C, Dosio A, Kjellström E, Chen Y, Hänsler A, Kupiainen M, Laprise R, Mariotti L, Maule CF, van Meijgaard E, Panitz HJ, Scinocca JF, Somot S (2018) The effects of 1.5 and 2 degrees of global warming on Africa in the CORDEX ensemble. *Environ Res Lett* 13:1–19. <https://doi.org/10.1088/1748-9326/aab1b1>
- Odoulami RC, Akinsanola AA (2017) Recent assessment of West African summer monsoon daily rainfall trends. *Weather* 99:1–4. <https://doi.org/10.1002/wea.2965>
- Phillips TJ, Gleckler PJ (2006) Evaluation of continental precipitation in 20th century climate simulations: the utility of multimodel statistics. *Water Resour Res* 42:W03202. <https://doi.org/10.1029/2005WR004313>
- Pokam MW, Longandjo GN, Moufouma-Okia W, Bell JP, James R, Vondou DA, Haensler A, Fotso-Nguemo TC, Guenang GM, Tchotchou ALD, Kamsu-Tamo PH, Takong RR, Nikulin G, Lennard CJ, Dosio A (2018a) Consequences of 1.5°C and 2°C global warming levels for temperature and precipitation changes over Central Africa. *Environ Res Lett* 13:1–12. <https://doi.org/10.1088/1748-9326/aab048>
- Pokam MW, Yontchang GD, Kamsu-Tamo PH, Kabengela H, Igru M, Tanessong R, Vondou DA, Guenang GM (2018b) Pathway of developing sub-seasonal to seasonal seamless prediction for disaster risk management over Central Africa. *S2S News Lett* 9:4–7
- Saha F (2015) Les changements climatiques et la vulnérabilité des villes d'Afrique centrale aux risques naturels : cas des inondations et des mouvements de masse à Bamenda (nord-ouest du Cameroun). *Edilivre-apis, Classique*, pp 206
- Sonwa DJ, Somorin OA, Jum C, Bele MY, Nkem JN (2012) Vulnerability, forest-related sectors and climate change adaptation: the case of Cameroon. *For Policy Econ* 23:1–9
- Sylla MB, Giorgi F, Coppola E, Mariotti L (2013) Uncertainties in daily rainfall over Africa: assessment of observation products and evaluation of a regional climate model simulation. *Int J Climatol* 33:1805–1817. <https://doi.org/10.1002/joc.3551>

- Sylla MB, Giorgi F, Pal JS, Gibba P, Kebe I, Nikiema M (2015) Projected changes in the annual cycle of high-intensity precipitation events over West Africa for the late twenty-first century. *J Clim* 28:6475–6488. <https://doi.org/10.1175/JCLI-D-14-00854.1>
- Tamoffo AT, Moufouma-Okia W, Pokam WM, Guenang GM, Vondou DA, Dosio A, Longandjo GN, Lennard CJ, Fotso-Nguemo TC, Nikulin G, Bell JP, Takong RR, James R, Haensler A, Tchotchou LAD, Kamsu-Tamo PH, Nouayou R (2018) Impacts of 1.5°C and 2°C global warming on moisture transport in the Central African region. *Clim Dyn* p Under Review
- Tanessong RS, Vondou DA, Djomou ZY, Igri PM (2017) WRF High resolution simulation of an extreme rainfall event over Douala(Cameroon): a case study. *Model Earth Syst Environ* 3:927–942. <https://doi.org/10.1007/s40808-017-0343-7>
- Taylor KE (2001) Summarizing multiple aspects of model performance in a single diagram. *J Geophys Res* 106:7183–7192
- Trenberth KE (2011) Changes in precipitation with climate change. *Clim Res* 47:123–138
- Vizy E, Cook KH (2012) Mid-twenty-first-century changes in extreme events over northern and tropical Africa. *J Clim* 25:5748–5767
- Zogning A, Ngouanet C, Ojuku T (2007) The catastrophic geomorphological processes in humid tropical Africa: a case study of the recent landslide disasters in Cameroon. *Sediment Geol* 199:13–17

## Affiliations

Denis Sonkoué<sup>1</sup>  · David Monkam<sup>2</sup> · Thierry C. Fotso-Nguemo<sup>1,3</sup> · Zéphirin D. Yepdo<sup>1,3</sup> · Derbetini A. Vondou<sup>1</sup>

<sup>1</sup> Laboratory for Environmental Modeling and Atmospheric Physics (LEMAP), Department of Physics, Faculty of Science, University of Yaounde 1, P.O. Box 812 Yaounde, Cameroon

<sup>2</sup> Department of Physics, Faculty of Science, University of Douala, P.O. Box 24157 Douala, Cameroon

<sup>3</sup> Climate Change Research Laboratory (CCRL), National Institute of Cartography, P.O. Box 157 Yaounde, Cameroon